Defense Special Weapons Agency
Alexandria, VA 22310-3398

DNA-TR-95-31

Three-Dimensional Analysis of Penetration into Geological Media

Mark A. Fry
Science Application Intl Corp
P.O. Box 1301
McLean, VA 22102

November 1996

Technical Report

CONTRACT No. DNA 001-91-C-0061

DESTRUCTION NOTICE:

Destroy this report when it is no longer needed.
Do not return to sender.

PLEASE NOTIFY THE DEFENSE SPECIAL WEAPONS AGENCY, ATTN: CSTI, 6801TELEGRAPH ROAD, ALEXANDRIA, VA 22310-3398, IF YOUR ADDRESS IS INCORRECT, IF YOU WISH IT DELETED FROM THE DISTRIBUTION LIST, OR IF THE ADDRESSEE IS NO LONGER EMPLOYED BY YOUR ORGANIZATION.

DISTRIBUTION LIST UPDATE

This mailer is provided to enable DSWA to maintain current distribution lists for reports. (We would appreciate your providing the requested information.)

☐ Add the individual listed to your distribution list.

☐ Delete the cited organization/individual.

☐ Change of address.

NOTE:
Please return the mailing label from the document so that any additions, changes, corrections or deletions can be made easily. For distribution cancellation or more information call DSWA/IMAS (703) 325-1036.

NAME: _____

ORGANIZATION: _____

OLD ADDRESS	CURRENT ADDRESS
_____	_____
_____	_____
_____	_____

TELEPHONE NUMBER: ( ) _____

DSWA PUBLICATION NUMBER/TITLE	CHANGES/DELETIONS/ADDITIONS, etc.) *(Attach Sheet if more Space is Required)*
_____	_____
_____	_____
_____	_____

DSWA OR OTHER GOVERNMENT CONTRACT NUMBER: _____

CERTIFICATION OF NEED-TO-KNOW BY GOVERNMENT SPONSOR (if other than DSWA):

SPONSORING ORGANIZATION: _____

CONTRACTING OFFICER OR REPRESENTATIVE: _____

SIGNATURE: _____

CUT HERE AND RETURN

DEFENSE SPECIAL WEAPONS AGENCY
ATTN: IMAS
6801 TELEGRAPH ROAD
ALEXANDRIA, VA 22310-3398

DEFENSE SPECIAL WEAPONS AGENCY
ATTN: IMAS
6801 TELEGRAPH ROAD
ALEXANDRIA, VA 22310-3398

REPORT DOCUMENTATION PAGE

Form Approved
OMB No. 0704-0188

1. AGENCY USE ONLY (Leave blank)	2. REPORT DATE	3. REPORT TYPE AND DATES COVERED
	961101	Technical 910425 - 941201

4. TITLE AND SUBTITLE
Three-Dimensional Analysis of Penetration into Geological Media

5. FUNDING NUMBERS
C - DNA 001-91-C-0061
PE - 62715H
PR - RS
TA - RC
WU - DH308350

6. AUTHOR(S)
Mark A. Fry

7. PERFORMING ORGANIZATION NAME(S) AND ADDRESS(ES)
Science Applications Intl Corp
P.O. Box 1303
McLean, VA 22102

8. PERFORMING ORGANIZATION REPORT NUMBER
SAIC-95/1009

9. SPONSORING/MONITORING AGENCY NAME(S) AND ADDRESS(ES)
Defense Special Weapons Agency
6801 Telegraph Road
Alexandria, VA 22310-3398
SPSD/Giltrud

10. SPONSORING/MONITORING AGENCY REPORT NUMBER
DNA-TR-95-31

11. SUPPLEMENTARY NOTES
This work was sponsored by the Defense Special Weapons Agency under RDT&E RMC Code B4662D RS RC SPSD 4300A 25904D.

12a. DISTRIBUTION/AVAILABILITY STATEMENT
Approved for public release; distribution is unlimited.

12b. DISTRIBUTION CODE

13. ABSTRACT *(Maximum 200 words)*

The Defense Special Weapons Agency's Conventional Weapons Effects Program requires state-of-the-art analysis of penetrator-target interaction. Science Applications International Corporation (SAIC) has conducted a program that applies sophisticated Eulerian codes to accurately capture the physics of the penetration process.

Penetration events are an important aspect of the interaction of non-nuclear munitions with structures. The penetrator exhibits near rigid body motion, at velocities below a few thousand feet per second, as it moves through the target producing a material boundary layer between the outer surface of the penetrator and the target material. These effects require codes that can maintain distinct material boundaries while advecting a solid with an attached boundary layer. In general, they can be simulated using both Lagrangian and Eulerian hydrocodes, but we have shown the robustness of using Eulerian codes for simulating the penetration event.

14. SUBJECT TERMS
Penetration
Benchmarking

15. NUMBER OF PAGES
16

16. PRICE CODE

17. SECURITY CLASSIFICATION OF REPORT	18. SECURITY CLASSIFICATION OF THIS PAGE	19. SECURITY CLASSIFICATION OF ABSTRACT	20. LIMITATION OF ABSTRACT
UNCLASSIFIED	UNCLASSIFIED	UNCLASSIFIED	SAR

CLASSIFIED BY:

N/A since Unclassified.

DECLASSIFY ON:

N/A since Unclassified.

SUMMARY

The Defense Special Weapons Agency's Conventional Weapons Effects Program requires state-of-the-art analysis of penetrator-target interaction. Science Applications International Corporation (SAIC) has conducted a program that applies sophisticated Eulerian codes to accurately capture the physics of the penetration process.

Penetration events are an important aspect of the interaction of non-nuclear munitions with structures. The penetrator exhibits near rigid body motion, at velocities below a few thousand feet per second, as it moves through the target producing a material boundary layer between the outer surface of the penetrator and the target material. These effects require codes that can maintain distinct material boundaries while advecting a solid with an attached boundary layer. In general they can be simulated using both Lagrangian and Eulerian hydrocodes, but we have shown the robustness of using Eulerian codes for simulating the penetration event.

A previous report (Fry *et al.*, 1993) documented simulations of the interaction of a weapon with buried structures performed in support of the TELL-91 test series conducted by DSWA in August and September, 1991. This report documents a study of the penetration of geologic material. Calculations were performed using SAIC's version of the HULL and CTH hydrocodes. Important physical models were included and validated using DSWA's set of penetration benchmarks..

CONVERSION TABLE

MULTIPLY	BY	TO GET
atmosphere (atm)	1013.25	millibar (mb)
centimeter (cm)	10^{-2}	meter (m)
foot (ft)	0.3048	meter (m)
gram (gm)	10^{-3}	kilogram (kg)
gram/centimeter^3 (g/cm^3)	10^3	kilogram/meter^3 (kg/m^3)
knot (kt)	0.51	meter/sec (m/s)
micron (μm)	10^{-6}	meter (m)
millibar (mb)	10^2	Newton/meter^2 (N/m^2)
millimeter (mm)	10^{-3}	meter (m)
Pascal (Pa)	1	Newton/meter^2 (N/m^2)
ton (t)	10^3	kilogram (kg)

TABLE OF CONTENTS

Section **Page**

SUMMARY iii

CONVERSION TABLE iv

FIGURES vi

BACKGROUND 1

1.1 BENCHMARKING 4
1.2 PRE-TEST ANALYSIS. 7

FIGURES

Figure Page

1-1 Important physical effects in penetration that affect computational modeling. 1
1-2 Benchmark #1 at 50 μsec. Left is steel density contours. Right is molten aluminum..... 4
1-3 Benchmark problem #1 at 225 msec. Left is steel density contour. Right shows molten aluminum..... 5
1-4 Benchmark problem #2 at 225 msec. Shown are density contours of steel and aluminum.. 6
1-5 Mass of molten aluminum versus time for benchmark problems 1 and 2..... 7
1-6 Benchmark problem #3. Steel projectile into soil at 280 msec. Time is 1 millisecond..... ...8

SECTION 1

BACKGROUND

Analytical efforts in penetration of geological material have relied mainly on empirically derived models. The very difficult problem of computing penetration from first principles has recently been rediscovered. Hydrocodes have performed very well at higher velocities, but at velocities below a few thousand feet per second, they have been shown to produce incorrect results. Figure 1-1 shows the important physical effects present during the penetration process. The thickness of the boundary layer has been exaggerated and is generally a few millimeters thick. Because it does not scale with penetrator size, it becomes exceedingly small compared to the size of a few hundred centimeter long I-2000. The time-dependent physics of this boundary layer forms the essence of the penetration problem. The high impedance provided by the high density penetrator along with its kinetic energy produce very high pressures in the target material surrounding the penetrator. As a result phase changes are likely to occur because of the localized, high temperatures. The non-linearity of the problem results from the coupling of momentum and energy into and out of the boundary layer as the penetrator encounters new target material.

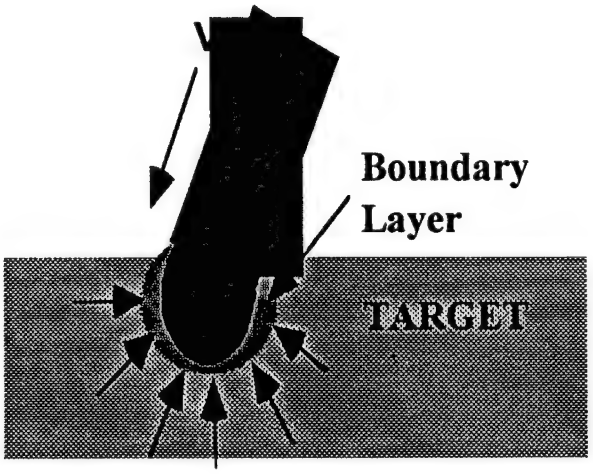

Figure 1-1. Important physical effects in penetration that affect computational modeling.

An equally important part of obtaining accurate penetration computations is the maintenance of the penetrator-target interface. For the case of rigid body motion, the penetrator does not deform, but does transfer energy and momentum to the target. In Eulerian codes, this interface must be preserved, as the grid is moved through the interface, or conversely, as the penetrator -target interface is moved through the grid. Artificial deformations due to mixing of penetrator and target material can create gradients which may lead to unwanted plastic flow of the penetrator. Some solutions tend to diffuse the interface over several grid points, which will result in penetrator deformation.

Our approach is to employ a boundary layer model that accounts for the heat from frictional and compressive stresses. We have chosen to couple this model to the advection or fluxing portion of an Eulerian, finite-difference code, the HULL code. The model is easily extended to other hydrocodes such as CTH. Within the boundary we solve in a first principles

manner the transfer of mass and momentum between the various states of the target material. This physical approach includes heat transfer. The heating which can lead to target/penetrator melting in the boundary layer is shown to have important effects on target damage.

However, because of the substantial 'passing through' of penetrator material in an Eulerian grid, uncertainties of the material interface defined by the penetrator and target are always present. We show improvements in this uncertainty by synergistically coupling the boundary layer into the advection algorithm. To accomplish this we utilize a new, boundary layer material. This material is produced when the original target material, e.g. soil, is crushed and reaches a threshold level where it then is physically altered.

The time-dependent physics of this boundary layer forms the essence of the penetration problem. The high impedance provided by the high density penetrator along with its kinetic energy produce very high pressures in the target material surrounding the penetrator. As a result phase changes are likely to occur because of the localized, high temperatures. The non-linearity of the problem results from the coupling of momentum and energy into and out of the boundary layer as the penetrator encounters new target material.

The force on the penetrator can be resolved into two components. The first is the normal force, similar to uniaxial stress which means the target responds along the material Huguenot. That is, there is a relationship between the stress and strain of the target material in compressive loading. This force is tied directly to the fluxing algorithm in the codes. No lateral forces are allowed.

The second is the tangential force determined by frictional forces at the penetrator-target interface. This force drives the boundary layer.

Our approach is to employ a boundary layer model that accounts for the heat from frictional and compressive stresses. This model is coupled to the advection or fluxing portion of the HULL code or other Eulerian codes. Within the boundary we solve in a first principles manner the transfer of mass and momentum between the various states of the target material. This physical approach includes heat transfer.

We model the boundary layer with a multi-phase approach. The 2-D mass continuity equations for the gaseous and solid particle phases of the boundary layer are given in equations (1.1) and (1.2). Material 1 is the gaseous or liquid matter, while material 2 is solid matter. The x- and y-velocities are u and v respectively, and the subscript denotes the phase being referred to, either gaseous or solid.

$$\frac{\partial \rho_1}{\partial t} + \frac{\partial (\rho_1 u_g)}{\partial x} + \frac{\partial (\rho_1 v_g)}{\partial y} = \Gamma \qquad (1.1)$$

$$\frac{\partial \rho_2}{\partial t} + \frac{\partial (\rho_2 u_p)}{\partial x} + \frac{\partial (\rho_2 v_p)}{\partial y} = -\Gamma \qquad (1.2)$$

Equations (1.3) and (1.4) are the conservation of momentum equations for the gaseous material in the x- and y-directions for 2-D flow. F_X and F_Y are the normal and tangential forces on the penetrator. Equations (1.5) and (1.6) represent the momentum conservation equations for the solid material.

$$\frac{\partial(\rho_1 u_g)}{\partial t}+\frac{\partial(\rho_1 u_g^{\,2}+\phi P_g)}{\partial x}+\frac{\partial(\rho_1 u_g v_g)}{\partial y}=-F_x+\Gamma u_p \tag{1.3}$$

$$\frac{\partial(\rho_1 v_g)}{\partial t}+\frac{\partial(\rho_1 u_g v_g)}{\partial x}+\frac{\partial(\rho_1 v_g^{\,2}+\phi P_g)}{\partial y}=-F_y+\Gamma v_p \tag{1.4}$$

$$\frac{\partial(\rho_2 u_p)}{\partial t}+\frac{\partial(\rho_2 u_p^{\,2})}{\partial x}+\frac{\partial(\rho_2 u_p v_p)}{\partial y}=F_x-\Gamma u_p \tag{1.5}$$

$$\frac{\partial(\rho_2 v_p)}{\partial t}+\frac{\partial(\rho_2 u_p v_p)}{\partial x}+\frac{\partial(\rho_2 v_p^{\,2})}{\partial y}=F_y-\Gamma v_p \tag{1.6}$$

The two energy conservation equations, for the gas and solid phase, are given in equations (1.7) and (1.8). Finally, the equation describing the conservation of the solid particle number density is shown in equation (1.9).

$$\frac{\partial(\rho_1 E_{gT})}{\partial t}+\frac{\partial(\rho_1 u_g E_{gT}+u_g\phi P_g)}{\partial x}+\frac{\partial(\rho_1 v_g E_{gT}+v_g\phi P_g)}{\partial y}=$$
$$\Gamma\left(\frac{u_g^2+v_g^2}{2}+E_{exothermal}+C_s\bar{T}_g\right)-(F_x u_g+F_y v_g)-\dot{Q} \tag{1.7}$$

$$\frac{\partial(\rho_2 E_{pT})}{\partial t}+\frac{\partial(\rho_2 u_g E_{pT})}{\partial x}+\frac{\partial(\rho_2 v_g E_{pT})}{\partial y}=$$
$$\dot{Q}+(F_x u_p+F_y v_p)-\Gamma\left(\frac{u_p^2+v_p^2}{2}+E_{exothermal}+C_s\bar{T}_p\right) \tag{1.8}$$

$$\frac{\partial N_p}{\partial t} + \frac{\partial (N_p u_p)}{\partial x} + \frac{\partial (N_p v_p)}{\partial y} = 0 \qquad (1.9)$$

However, because of the substantial 'passing through' of penetrator material in an Eulerian grid, uncertainties of the material interface defined by the penetrator and target are always present. We show improvements in this uncertainty by synergistically coupling the boundary layer into the advection algorithm. To accomplish this we utilize a new, boundary layer material. This material is produced when the original target material, e.g. soil, is crushed and reaches a threshold level where it then is physically altered. Figure 1-2 shows an example of the use of this model.

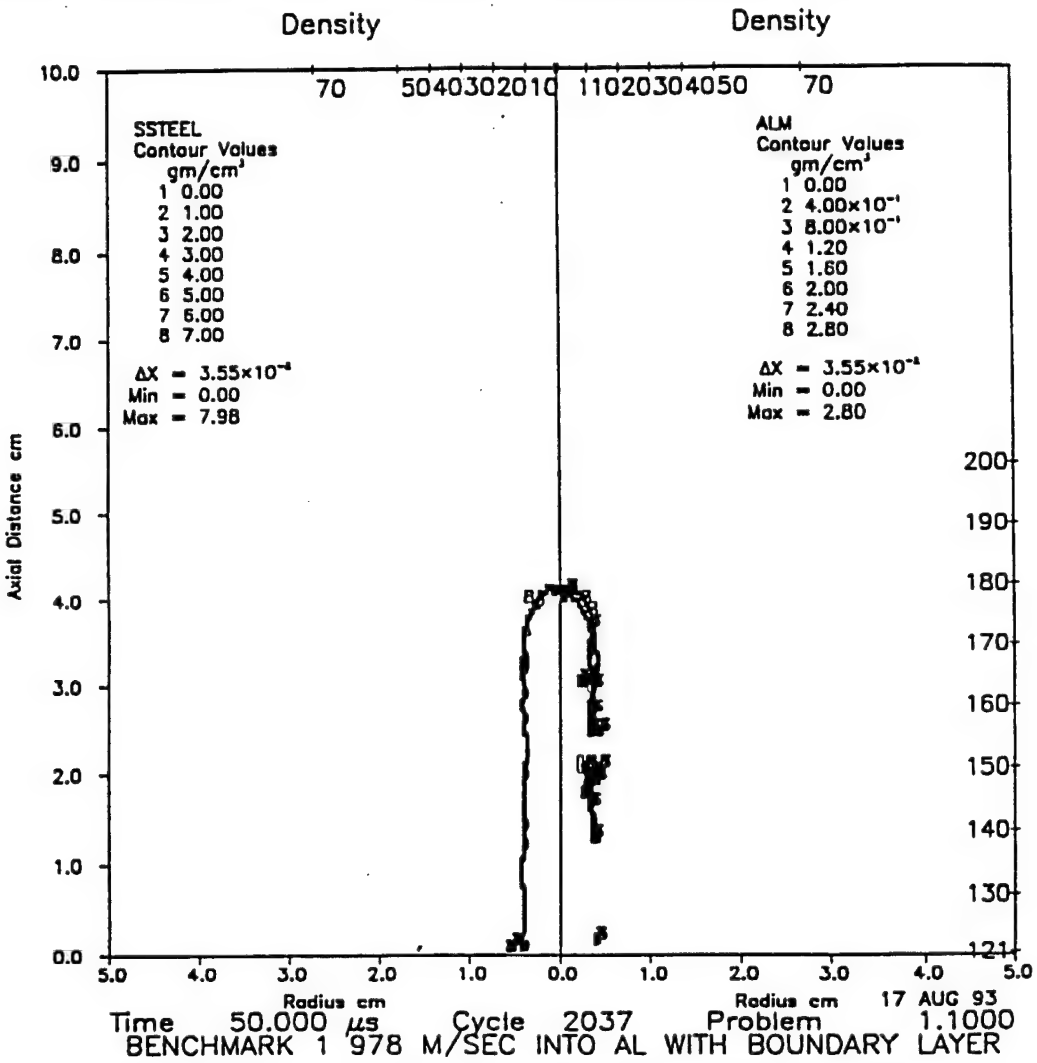

Figure 1-2. Benchmark #1 at 50 μsec. Left is steel density contours. Right is molten aluminum.

1.1 BENCHMARKING.

Previously we have employed the above model to penetration events that have been experimentally investigated. Forrestal et al. (1992) has carried out steel projectile into aluminum target experiments. They measured the penetration depth, hole size, observed the post-test

penetrator condition. Additionally, they assessed the constitutive properties of the aluminum targets. These experiments used a high strength steel penetrator, VESCOMAx, static yield strength >1500 MPa against soft aluminum targets with yield strengths ~ 500 MPa. Our results have shown very good agreement with these experiments as shown in Table 1-1.

Table 1-1.

Comparison of laboratory measurements of projectile penetration versus simulation.

Projectile velocity	Shape	Penetration Depth Measured	Calculated	Percent Diff
978 m/sec	Ogive	127cm	115	9%
959 m/sec	Round	109cm	105	4%

In addition, we ran lower velocity projectiles both in 2-D and 3-D. The results presented above are shown in graphical form in Figures 1-2 - 1-4.

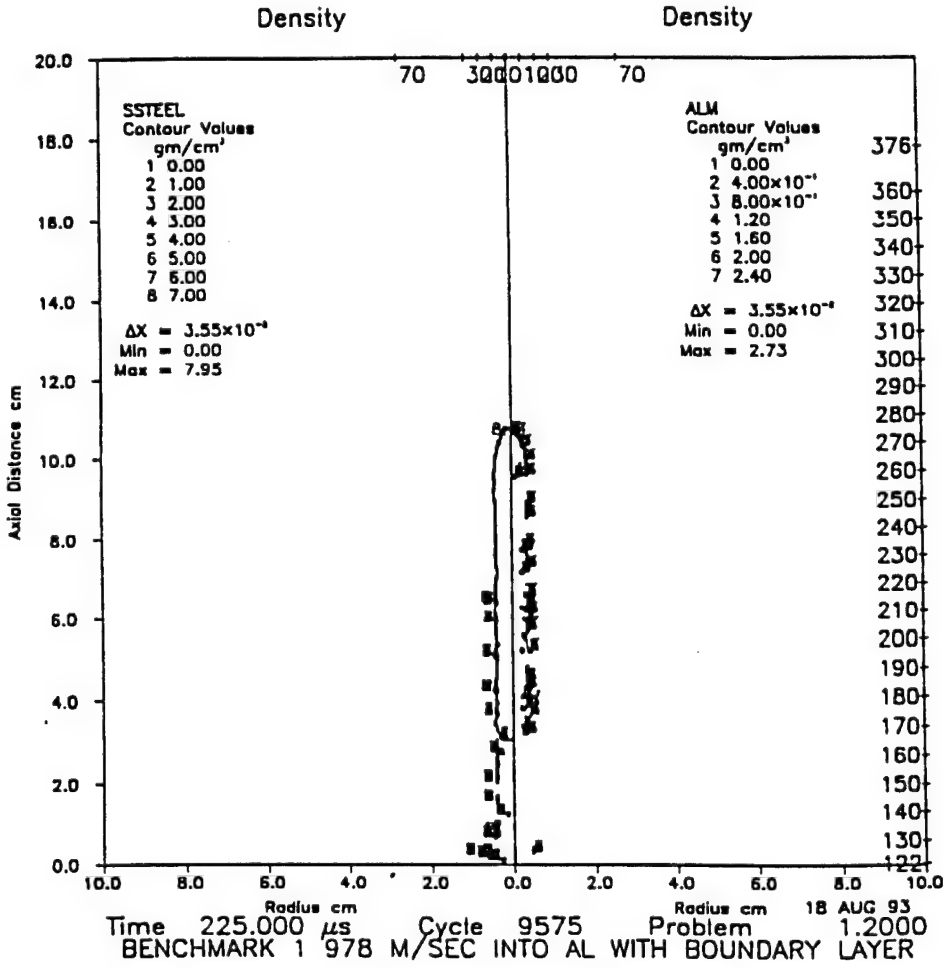

Figure 1-3. Benchmark problem #1 at 225 msec. Left is steel density contour. Right shows molten aluminum.

Figure 1-2 shows a HULL calculation at 50 microseconds. Problem 1 with the ogive nose and velocity of 978 m/sec is shown in density contours of steel (on left) and molten aluminum (on right). Notice the molten aluminum inside the crater. Figure 1-3 shows similar contours at t=225 μ sec. The projectile has almost come to a halt at about 11 cm depth into the aluminum block. Figure 1-4 shows the second benchmark problem at 225 μ sec. The rounded nose penetration melts more aluminum than the ogive. Figure 1-5 shows a comparison of the two calculations with mass versus time being plotted. Only a small amount of mass actually reaches the molten state.

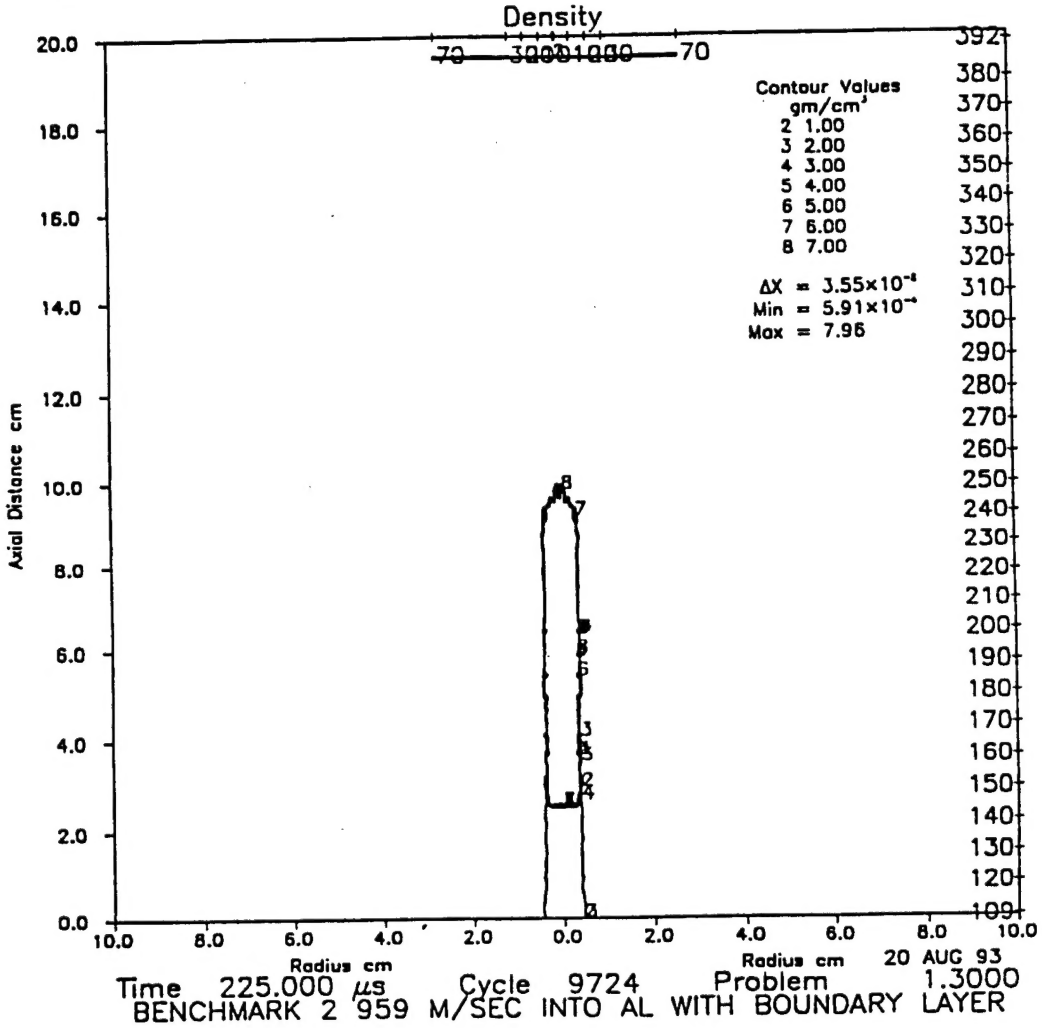

Figure 1-4. Benchmark problem #2 at 225 msec. Shown are density contours of steel and aluminum.

In Figure 1-6 we show density contours for benchmark problem 3 where a steel projectile penetrates soil at 280 m/sec. Notice the interface can be defined on a cell by cell basis.

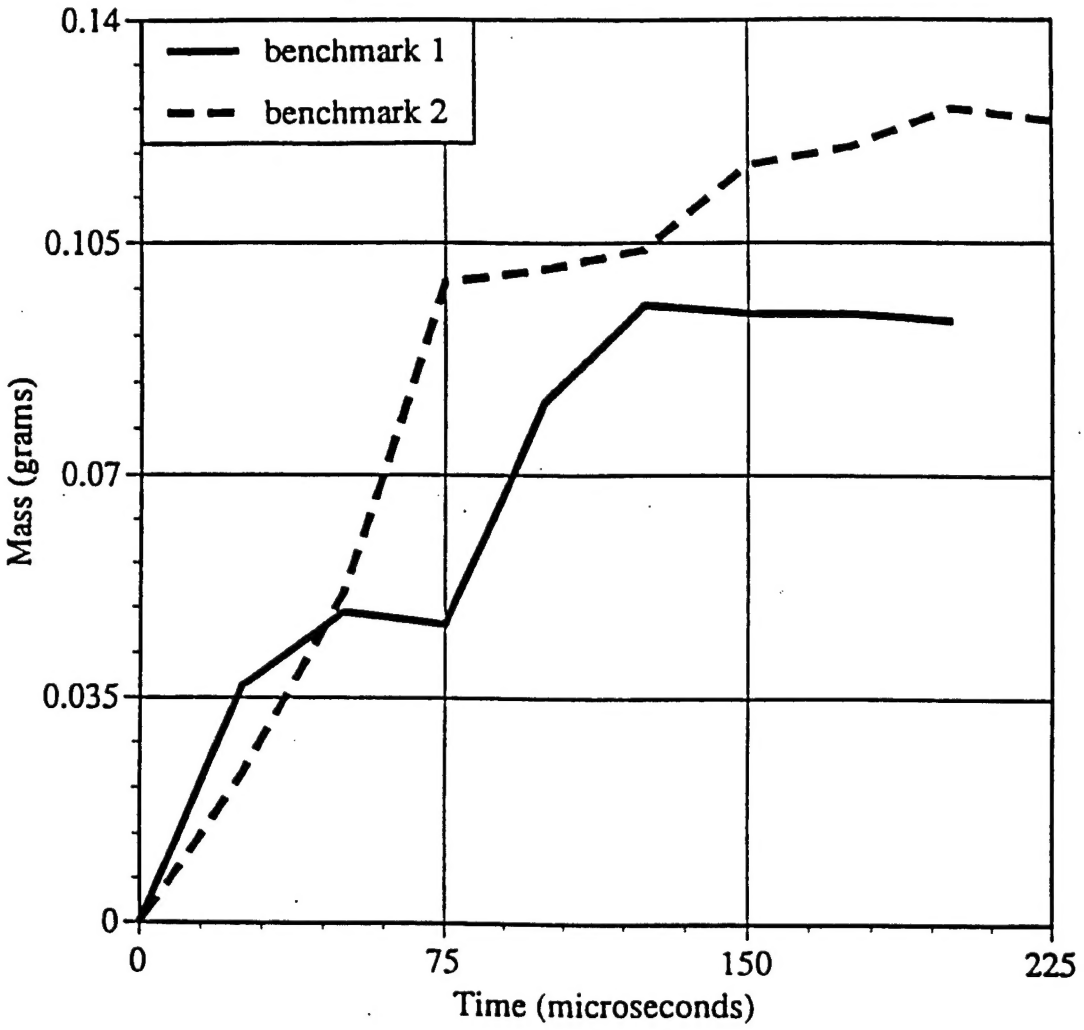

Figure 1-5. Mass of molten aluminum versus time for benchmark problems 1 and 2.

1.2 PRE-TEST ANALYSIS.

SAIC performed 2-D and 3-D analysis to support the CWE program. These calculations of the model targets composed of soil, concrete, sand, and other geological materials. Test events from the Dipole Series were simulated as per the test specifications. 1-D calculations were performed to understand the uncertainties in the material models. For example, the soil bacilli is usually characterized with laboratory tests. The data was acquired and used to build the best possible constitutive material models. Often there is no reported uncertainties associated with these measurements. To understand what would occur if there were variations, SAIC conducted parameter studies to characterize our numerical material model uncertainties. These studies utilized WONDY.

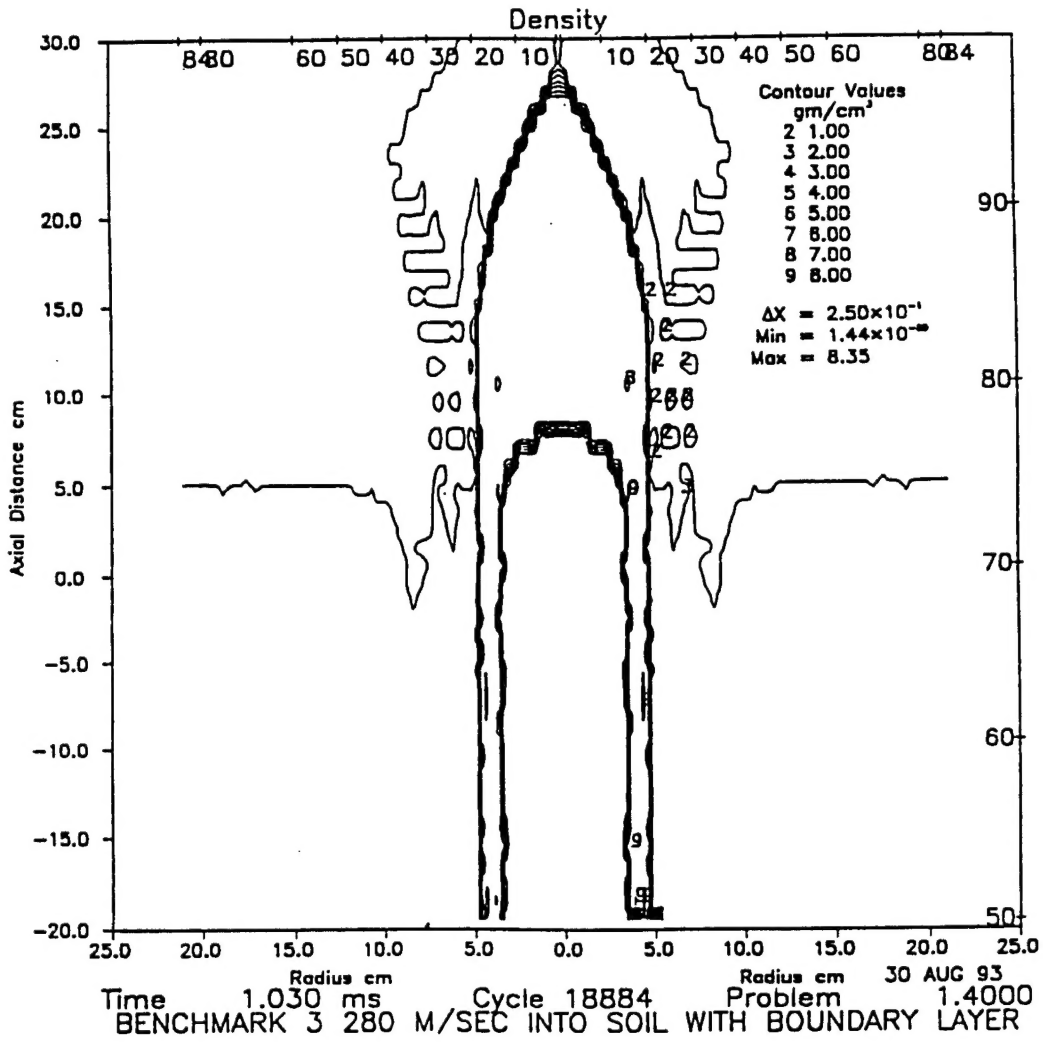

Figure 1-6. Benchmark problem #3. Steel projectile into soil at 280 m/sec. Time is 1 millisecond.

Differences between pre-test predictions and test results were addressed by examining the weaknesses in the codes and/or models. Sensitivity studies that consist of varying the controlling elements of the models were performed. These elements included material models, both for the target and penetrator, the advection algorithm, and the boundary layer.

The final depth of penetration, hole size, and projectile deformations are recorded for every test; there are no differential measurements as the penetrator moves through the target. Therefore, the main guidelines for comparisons are the final depth and projectile deformation, if any.

We assume that the initial impact velocity, angle of impact, and geometrical description of the penetrator will be accurately known. If pre-test comparisons are not found to be inadequate, the material models for the penetrator and target will first be examined. The advection algorithm together with the boundary layer formulation will then be investigated. Calculations with improvements will be made.

DISTRIBUTION LIST

DSWA-TR-95-31

DEPARTMENT OF DEFENSE

DEFENSE INTELLIGENCE AGENCY
ATTN: DIW-4
ATTN: G WEBER

DEFENSE SPECIAL WEAPONS AGENCY
2 CY ATTN: ISST

DEFENSE TECHNICAL INFORMATION CENTER
2 CY ATTN: DTIC

FIELD COMMAND DEFENSE SPECIAL WEAPONS AGENCY
ATTN: FCTO
ATTN: DR BALADI

DEPARTMENT OF THE ARMY

U S ARMY ENGR WATERWAYS EXPER STATION
ATTN: F DALLRIVA

DEPARTMENT OF THE NAVY

NAVAL RESEARCH LABORATORY
ATTN: CODE 5227 RESEARCH REPORT

DEPARTMENT OF THE AIR FORCE

AIR UNIVERSITY LIBRARY
ATTN: AUL-LSE

OTHER GOVERNMENT

CENTRAL INTELLIGENCE AGENCY
ATTN: OSWR/NED

DEPARTMENT OF DEFENSE CONTRACTORS

APTEK, INC
ATTN: T MEAGHER

GENERAL ATOMICS, INC
ATTN: CHARLES CHARMAN

HORIZONS TECHNOLOGY, INC
ATTN: B KREISS
ATTN: B LEE

INSTITUTE FOR DEFENSE ANALYSES
ATTN: CLASSIFIED LIBRARY

KAMAN SCIENCES CORP
ATTN: VERNON SMITH

KAMAN SCIENCES CORPORATION
ATTN: DASIAC

LOGICON R AND D ASSOCIATES
ATTN: LIBRARY

SCIENCE APPLICATIONS INTL CORP
2 CY ATTN: M A FRY

SRI INTERNATIONAL
ATTN: M SANAI

TITAN CORPORATION (THE)
ATTN: R ENGLAND

WEIDLINGER ASSOC, INC
ATTN: H LEVINE

WEIDLINGER ASSOCIATES, INC
ATTN: RAYMOND DAJAZZIO